Cellulose (2019) 26:3987–4004
https://doi.org/10.1007/s10570-019-02354-8

ORIGINAL RESEARCH

Synthesis, microstructure transformations, and long-distance inductive effect of poly(acrylethyltrimethylammonium chloride) cotton with super-high adsorption ability for purifying dyeing wastewater

Chunli Song · Hongyan Li · Yikai Yu

Received: 6 October 2018 / Accepted: 27 February 2019 / Published online: 5 March 2019

Abstract A new poly(acrylethyltrimethylammonium chloride) cotton with flexible long-chain cations was prepared by surface polymerization of acrylethyltrimethylammonium chloride and grafting cotton with unsaturated bonds at 50 °C for 1.5 h. A series of microstructure transformations of poly(acrylethyltrimethylammonium chloride) cotton adsorption were first observed by Fourier transform infrared spectroscopy, X-ray photoelectron spectroscopy, and X-ray diffraction technologies. It was discovered that a long-distance flexible inductive effect occurred during poly(acrylethyltrimethylammonium chloride) cotton adsorption, causing a highly efficient purification ability for treating dyeing wastewater. The adsorption capacity of poly(acrylethyltrimethylammonium chloride) cotton was 292.18 and 2702.70 times higher than that of the widely used activated carbon and common natural cotton, respectively. In addition, poly(acrylethyltrimethylammonium chloride) cotton achieved the relatively good recyclability with a desorption technology and it was the first realization of self-purification of the desorption waste solution in a recycling application to avoid secondary pollution.

Co-first authors: Chunli Song and Hongyan Li.

C. Song · H. Li · Y. Yu (✉)
College of Chemistry and Chemical Engineering, Jiangxi Normal University, Ziyang Road 99, Nanchang 330022, China
e-mail: yuyikai1980@163.com

Y. Yu
Key Laboratory of Chemical Biology of Jiangxi Province, Ziyang Road 99, Nanchang 330022, China

Graphical abstract

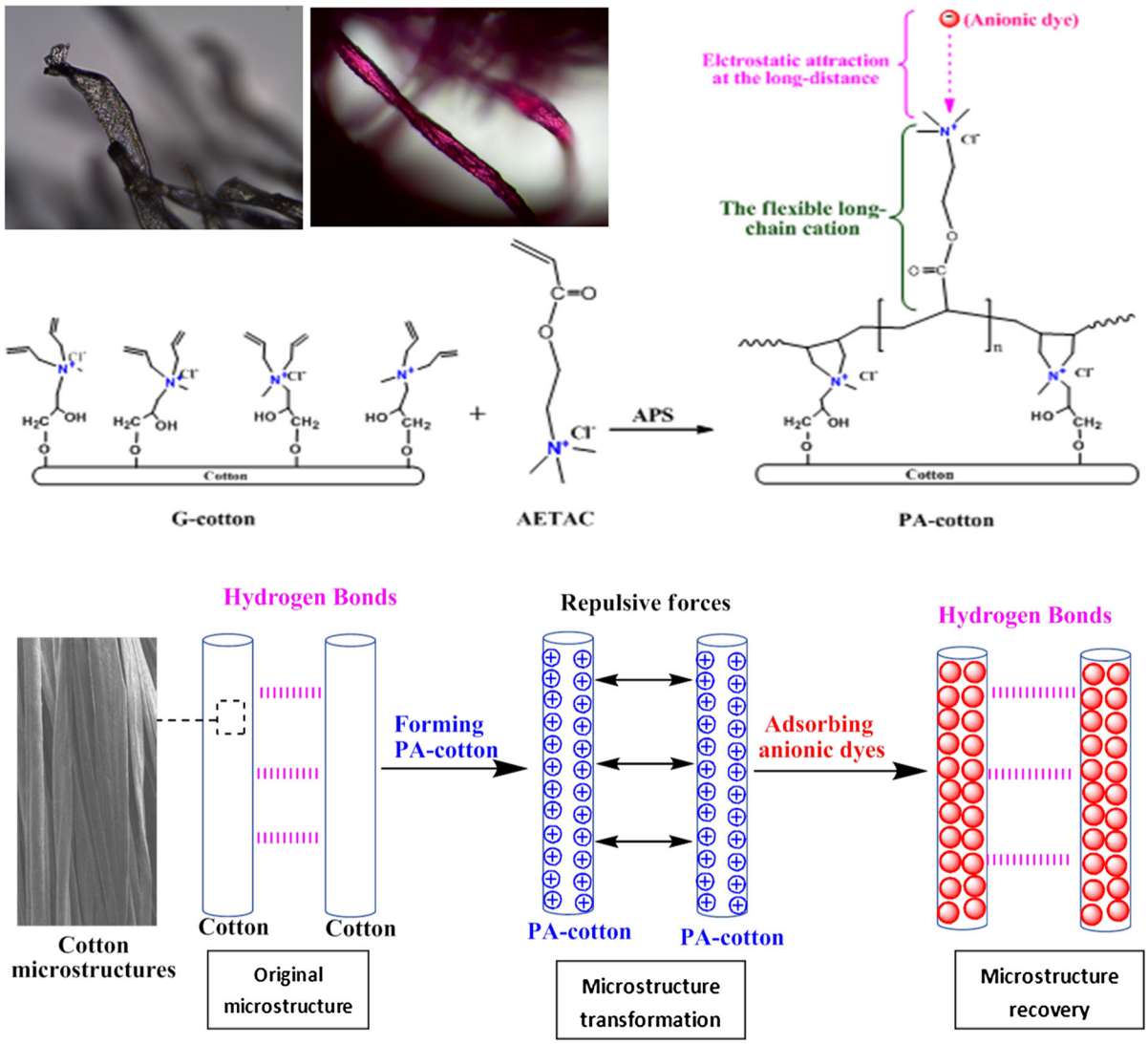

Keywords Super-high adsorption capacity · Cotton adsorbent · Microstructure transformation · Long-distance induction · Flexible induction · Dyeing wastewater · Self-purification

Introduction

Dyeing wastewater containing harmful dyes is one of the main water pollution sources around the globe (An et al. 2016; Li et al. 2017; Toprak and Anis 2017; Zereshki et al. 2018). Adsorption is regarded as one of the most simple and practical methods for purifying wastewater and it is the key to selecting suitable adsorbents (Agbovi et al. 2017; Goel et al. 2015; Kumar et al. 2018; Natarajan et al. 2018; Samaneh et al. 2017; Shao et al. 2017; Zhang et al. 2016, 2017). At present, activated carbon is still the most commonly used adsorbent material for water purification. It has been proven that activated carbon can provide efficient adsorption of certain small dyes in dyeing wastewater through the aid of its specific structures of porosity, network, and large specific surface (Aschermann et al. 2018; Gupta et al. 2011; Hadi et al. 2015; Lompe et al. 2016; Mccleaf et al. 2015). However, it is not ideal for

activated carbon to adsorb large dyes or other large pollutants because its pore size is so small. Therefore, it has usually been adopted to combine activated carbon with expensive and toxic oxidizing substances (e.g., ClO_2, CuO, Fe_2O_3, V_2O_5, and Fenton reagent). This treatment can decompose the large dyes, after which they can be adsorbed by activated carbon (Ansari et al. 2016; Chaudhary et al. 2016; Suresh et al. 2014; Wang et al. 2010), resulting in an increase in application cost and secondary pollution. In addition, the difficult waste disposal of used activated carbon is also a main factor preventing wide applications of activated carbon. Therefore, we aimed to develop new adsorbent materials to treat dyeing wastewater more efficiently.

To date, there are some concerns with using natural adsorbent materials for purifying dyeing wastewater (Lu et al. 2018). Cotton is one of the most abundant and environmentally friendly natural polymers. Cationic cotton is known as a functional cotton derivative, which can produce electrostatic attractions with anionic dyes by its cationic groups and is usually applied to improve the uptake of anionic dyes (Toprak et al. 2018; Wang et al. 2009). In fact, this result is due to the improvement in the adsorption ability of cationic cotton toward the anionic dye. Meanwhile, we estimate that the adsorbent materials derived from the cationic modification of cotton will have the following unique application advantages over existing adsorbents: (1) Cotton can be directly adaptable to dyeing conditions (when being dyed) and can be directly used in the dyeing vat for purifying dyeing wastewater at the dyeing source. (2) Cotton has the weaving function of textile fibres and the cotton-modified materials can be processed into a variety of practical water treatment products, e.g., adsorption interception fabrics, adsorption non-woven fabrics, and industrial sewage filters. Therefore, we believe that cationic cotton will be a good new adsorbent candidate. However, conventional grafted cationic cottons have not been widely used in wastewater treatment because their cationic degrees are too low.

Our previous investigations successfully developed a series of new polycationic cotton adsorbents with relatively high cationic degrees, i.e., polycationic film coated cotton (PF-cotton, poly(dimethyldiallylammonium chloride) cotton chemical structure) (Jia et al. 2017), long-chain alkylation poly(tetradecylallyldimethylammonium chloride) cotton (LP-cotton) (Song et al. 2018), and multidimensional cationic poly(triallylmethylammonium chloride) cotton (PT-cotton) (Song et al. 2018, in press). These cotton-modified cotton adsorbents have relatively high adsorption capacities for purifying dyeing wastewater when compared to existing adsorbent materials, which are 17.4–145.3 times higher than that of the widely-used activated carbon (Jia et al. 2017; Song et al. 2018a, b, in press). However, it is still a research goal to continuously improve the adsorption abilities of the cotton-modified adsorbents. Our next research goal is further improvement of the cationic properties on the cotton surface. In previous work, we noticed that the five-ring cations in PF-cotton and PT-cotton were very rigid and the long-chain alkylation cations in LP-cotton were highly affected by steric hindrance, suggesting that the mobile activity of those cations appeared relatively weak. Therefore, there is potential for increasing the mobile activities of the cations so as to improve the combination frequency between the cations and the anionic dyes. In view of this new problem, we deduce that if some flexible cations with high mobile activities can be incorporated into cotton, it will become easier for the cations to quickly catch the anionic dyes in water, thus improving the adsorption capacities and rates of the obtained cotton-modified adsorbents. This new idea has caused us to continuously explore further cationic modification of cotton for purifying dyeing wastewater more efficiently than could be done before.

In this work, we further designed a new poly(acrylethyltrimethylammonium chloride) cotton (PA-cotton) with flexible long-chain cations through surface co-polymerization of one monomer containing a flexible long-chain cation (i.e., acrylethyltrimethylammonium chloride, AETAC) and another grafted cotton with unsaturated bonds (G-cotton). When the PA-cotton obtained was used as the adsorbent for dealing with dyeing wastewater, the incorporated cations were flexible, having high enough mobile activities to increase the combination frequencies with the anionic dyes. Moreover, the distance between the cations and the cotton surface was lengthened by the long-chain linkage, making it possible for the cations to probe a far distance into the water to catch the anionic dyes without hindrance (Scheme 1). Thus, the long-distance flexible inductive effect would significantly raise the adsorption capacity and rate of PA-cotton. In addition, a series of microstructure

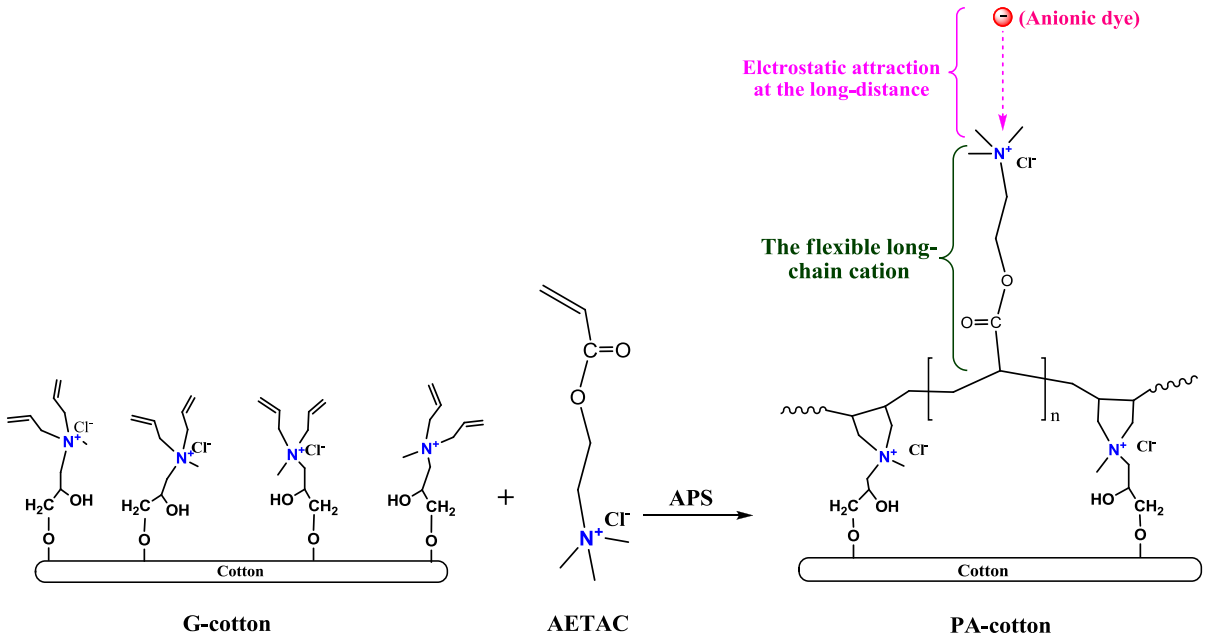

Scheme 1 Synthesis of the new PA-cotton adsorbent and its possible long-distance flexible inductive effect to adsorb anionic dyes in water

transformations of PA-cotton adsorption were first observed by Fourier transform infrared spectrum (FTIR), X-ray photoelectron spectroscopy (XPS), and X-ray diffraction (XRD) technologies to further investigate the PA-cotton adsorption behaviours for purifying dyeing wastewater.

Experiment

Materials

Cotton raw materials were 100% pure cotton fabrics, which were supplied from Jiangsu Nantong Si'ente Chemical Co., Ltd (China), weighting: 130 g/m^2, yarn density: 40. Reactive Scarlet 3BS is an industrial purity product and was also supplied from Jiangsu Nantong Si'ente Chemical Co., Ltd (China). AETAC was purchased from Shandong Luyue Chemical Co., Ltd (China). Ammonium persulfate (APS) was purchased from Yixing Tianpeng Fine Chemical Co., Ltd (China).

Method

G-cotton synthesis

G-cotton was synthesized under the same conditions as that used when 3-chloro-2-hydroxypropylmethyldiallylammonium chloride is grafted with triethanolamine-treated 100% cotton fabric in a NaOH solution based on our previous study (Jia et al. 2017).

Synthesis of PA-cotton

First, 0.5 g of G-cotton was dispersed in 15 mL of deionized water in a 50 mL round-bottomed flask. Then, 0.75 g of AETAC and 0.5 g of APS initiator were added and the reaction mixture was stirred at 50 °C for 1.5 h to form poly(acrylethyltrimethylammonium chloride) cotton (PA-cotton). The solid PA-cotton was fully washed with 50 mL of 40 °C water 3 times to remove the by-products of homo-polymers of AETAC on the PA-cotton surface. The PA-cotton was dried under vacuum at 50 °C to be reserved.

Adsorption studies of PA-cotton samples

The adsorption experiments were conducted with selection of a large anionic dye (i.e., Reactive Scarlet 3BS, Scheme 2) as the test object. The adsorption behaviour of PA-cotton toward the dye was determined by immersing different dosages (ranging from 0.001 to 0.01 g) of PA-cotton into 10 mL of a 100 mg/L dye solution of Reactive Scarlet 3BS at 30 °C. After adsorbing for 100 h, the PA-cotton was separated by filtration using a medium-speed filter paper to timely detect the adsorption results. The dye concentrations of the solutions before and after PA-cotton adsorption were determined with a spectrophotometer, which can be used to evaluate the adsorption ability of PA-cotton. Subsequently, the adsorption effect of PA-cotton at different times was investigated as follows: 0.01 g of PA-cotton samples were immersed in 10 mL of a 100 mg/L dye solution of Reactive Scarlet 3BS at 30 °C for 1–8 min with continuous stirring and a spectrophotometer was used to analyse the adsorption result at each time interval (t). In addition, the adsorption effect of PA-cotton at different temperatures was further investigated as follows: 0.002 g of PA-cotton samples were immersed in 10 mL of a 100 mg/L dye solution of Reactive Scarlet 3BS at 30–50 °C for 100 h with continuous stirring, followed by filtration. A spectrophotometer was used to detect the adsorption results at different temperatures.

Measurement

The degree of substitution (DS) was defined as the average number of cationic units substituted onto each hydroxyl group in the D-glucose unit of the cotton cellulose. DS values of PA-cotton consisted of the number values of the cationic units in the starting material of G-cotton [(DS_0, which had been measured to be 0.065 in our previous work (Jia et al. 2017)] and the number values of the cationic AETAC units (DS_1), which could be measured with an elemental analysis method. An Arvato EA 3000 Elemental Analyzer was used to measure the nitrogen content of the obtained samples, which could be used to calculate the average molar number (n) of N-containing cationic units in each mole of the D-glucose unit of cotton cellulose because the molar number of nitrogen is equal to those of the cationic units. Subsequently, the molar numbers of nitrogen elements (n) were directly divided by the molar numbers of hydroxyl groups in each D-glucose unit of cotton cellulose (there were 3 hydroxyl groups in each D-glucose unit of cotton cellulose) to calculate the DS values of PA-cotton. The formulas for calculating the DS values of PA-cotton are shown in Eq. 1 as follows:

$$DS = DS_0 + DS_1 = 0.065 + DS_1 = n/3 \quad (1)$$

FT-IR measurements were recorded on a Nicolet FT-IR (510 P, USA) spectrophotometer using the disk method within the wavelength range of 4000–400 cm^{-1}.

XPS measurements were carried out with a Thermo VG multilab 2000 spectrometer with an Al Ka X-ray source.

The crystallinity of PA-cotton was measured by XRD analysis with a Rigaku D/MAX-IIA X-ray diffractometer using CuKα radiation at 30 kV and 20 mA, and the diffractograms were recorded at room temperature over the range of 2θ = 10°–90°.

Optical microscope photos for PA-cotton adsorption in water were observed with a 35TV optical microscope instrument with a computer camera.

The colour differences (ΔE) before and after PA-cotton adsorption and desorption could be accessed by measuring the values of ΔL, Δa, and Δb in a CIELAB color space, using a Gretag Macbeth Color EYE^R 3100 Instrument, and were calculated based on the following equation, i.e.,

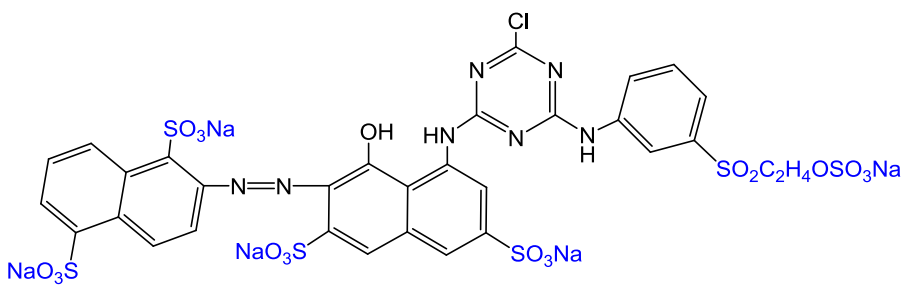

Scheme 2 The chemical structure of the large water soluble dye Reactive Scarlet 3BS

$$\Delta E = \left(\Delta L^2 + \Delta a^2 + \Delta b^2\right)^{1/2} \quad (2)$$

The maximum absorbance–wavelength of the selected dye solution (588 nm, Reactive Scarlet 3 BS) was determined with a U-3310 UV–Vis spectrophotometer. At the maximum absorbance–wavelength of 588 nm, the dye absorbance in the untreated solution (A_0) and in the PA-cotton treated solution (A_t) were measured with a Shanghai 721 spectrophotometer. The dye removal percentage (R%) was calculated from the percentage absorbance using the following equation (Eq. 3):

$$R(\%) = \frac{A_0 - A_t}{A_0} \times 100\% \quad (3)$$

The Cu^{2+} concentrations before and after the interactions between the desorption waste solution of PA-cotton desorption and $CuSO_4$ were determined with a plasma optical emission spectrometer (725-ES, Varian Co. Ltd, USA). The Cu^{2+} removal percentage (R′%) was calculated using the following equation (Eq. 4):

$$R'\% = \frac{C_0 - C_1}{C_0} \times 100\% \quad (4)$$

where C_0 is the Cu^{2+} concentration in the original $CuSO_4$ solution and C_1 is the Cu^{2+} concentration after the interactions between the desorption waste solution of PA-cotton desorption and the $CuSO_4$ solution.

Results and discussion

Optimization of PA-cotton preparation

The new poly(acrylethyltrimethylammonium chloride) cotton (PA-cotton) was synthesized by surface co-polymerization of one monomer containing a flexible long-chain cation (i.e., AETAC) and another grafted cotton with unsaturated bonds (G-cotton). The effects of the different reaction conditions (reaction temperature, AETAC amount, initiator amount, and reaction time) on PA-cotton synthesis were systemically investigated to optimize the conditions for PA-cotton preparation (Fig. 1). The effects of each condition were evaluated by the cationic DS values and the adsorption abilities of the obtained PA-cotton samples. The results showed that the dye removal percentage (R%) of the PA-cottons increased with the increase in the cationic DS (Fig. 1a). Moreover, when the DS values of PA-cottons were above 0.16, all R% values were > 99% (Fig. 1b–d), which further confirmed that the higher DS values of PA-cottons would give better adsorption abilities. Meanwhile, according to the relationships in Eq. 1 (i.e., DS = DS_1 + 0.065), the higher DS values of PA-cotton indicated higher numbers (DS_1) of the AETAC units in the structures of PA-cotton, while the flexible long-chain cations were included in the AETAC units. Thus, the above results suggest that the better adsorption abilities of PA-cotton could be derived from the effect of the higher numbers of flexible long-chain cations in the structures of PA-cotton, i.e., the flexible long-chain cations played successful roles in improving the adsorption abilities of PA-cotton.

Thus, we confirmed the most mild conditions as far as possible by which the highest DS value of the PA-cotton could be obtained, as the optimum preparation conditions for PA-cotton preparation: 50 °C reaction temperature, 1.5/1 weight ratio of AETAC/G-cotton, 1/1 weight ratio of the initiator (APS)/G-cotton, and 1.5 h reaction time. The optimal cationic DS of PA-cotton should be 0.32, which was 4.78, 4.64, 2.96, and 2.48 times higher than that of the similar G-cotton, PF-cotton, LP-cotton, and PT-cotton in our previous work, respectively (Table 1) (Jia et al. 2017; Song et al. 2018, 2019), showing a super-high DS value.

Structure analysis of PA-cotton

The structure of the PA-cotton obtained was analysed by FT-IR and the result is shown in Fig. 2. Similar to the untreated cotton (Curve “A” in Fig. 2), the FT-IR spectra of the PA-cotton (Curve “B”) shows the absorption of cotton skeletons at 1029–1160 cm^{-1} (Peak 1), 1431 cm^{-1} (Peak 2), 1640 cm^{-1} (Peak 3), 2900 cm^{-1} (Peak 5), and 3348 cm^{-1} (Peak 6). Moreover, compared to the FT-IR spectra of the untreated cotton (Curve “A”), the spectra of the PA-cotton shows a new absorption of C=O at 1736 cm^{-1} (Peak 4), which is attributed to the ester linkage in the AETAC unit of PA-cotton. Therefore, the structure of PA-cotton was as expected. In addition, there was clear information that the FT-IR absorption of C=O at 1736 cm^{-1} attributed to the ester linkage in the AETAC unit was greatly decreased after PA-cottons adsorbed the coloured dyes in the water (Peak 4 in Curve “C” versus that in Curve “B”), while other FT-

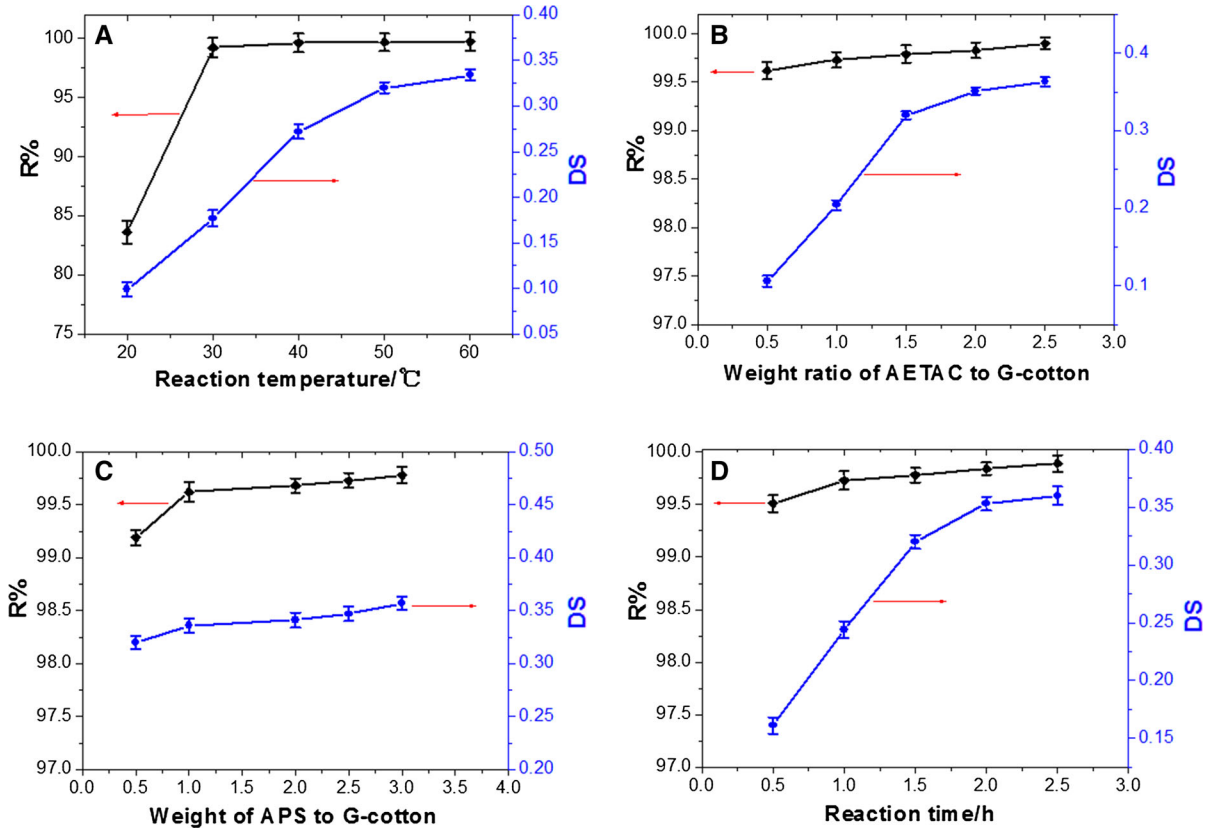

Fig. 1 Optimization of PA-cotton preparation. **R%*: the dye removal percentage (0.01 g PA-cotton was added to 10 mL of a 100 mg/L dye solution of Reactive Scarlet 3BS at 30 °C for 100 h)

Table 1 Comparison of DS values of PA-cotton to several similar cotton-modified adsorbents developed in our previous work

Adsorbent	DS value	References
G-cotton	0.067	Jia et al. (2017)
PF-cotton	0.069	Jia et al. (2017)
LP-cotton	0.108	Song et al. (2018)
PT-cotton	0.129	Song et al. (2019)
PA-cotton	0.320	This work

IR absorptions of the cotton skeletons changed little, suggesting that the AETAC unit of PA-cotton had a sensibility to adsorb the dyes in water, indicating its structure underwent a clear transformation after adsorbing the dyes.

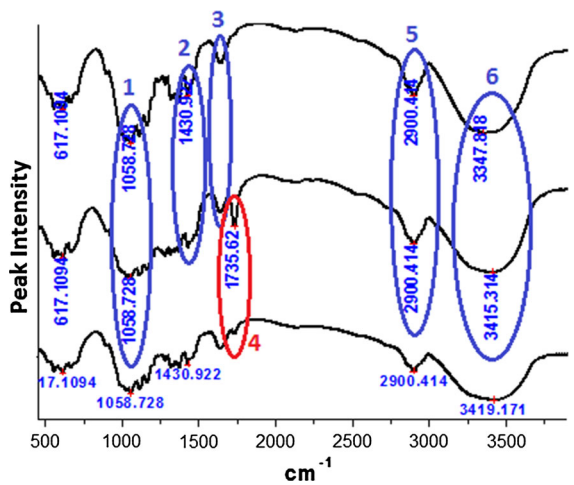

Fig. 2 Comparing the FT-IR analysis of untreated cotton (A), PA-cotton before (B) and after (C) adsorbing the dyes

Comparing the adsorption capacity and rate of PA-cotton

Based on the experimental procedure in "Adsorption studies of pa-cotton samples" section, the adsorption behaviours of PA-cotton toward the selected dye (Reactive Scarlet 3BS) were determined by immersing different dosages (ranging from 0.001 to 0.01 g) of PA-cotton in 10 mL of a 100 mg/L dye solution of Reactive Scarlet 3BS at 30–50 °C to adsorb for 100 h. The results are shown in Fig. 3a–c.

Figure 3a–c shows that the dye removal percentages increased with the increase in PA-cotton dosages and the adsorption temperature. At 30 °C, there was a satisfactory dye removal percentage (99.14%) achieved at a low PA-cotton dosage of 0.003 g (Fig. 3a), while the satisfactory dye removal percentages of 95.38% and 96.46% could be achieved at the lower dosages of 0.002 g under adsorption temperatures of 40 °C (Fig. 3b) and 50 °C (Fig. 3c), respectively. The adsorption data at the saturated adsorption states at dosages of 0.001–0.003 g at 30 °C were substituted into the Langmuir equation, and the maximal adsorption capacity (Q_{max}) of PA-cotton was calculated from the intercept of the linear plot of this equation. Here, the Q_{max} of the PA-cotton at 30 °C was 540.54 mg g^{-1}. Several typical and similar adsorbents were further selected to compare the superiority of PA-cotton adsorption capacity and rate, whose test conditions were the same as the PA-cotton adsorption in this work. The results are listed in Table 2. The adsorption capacity of PA-cotton was 292.18 and 2702.70 times higher than that of the widely-used activated carbon and the common untreated cotton

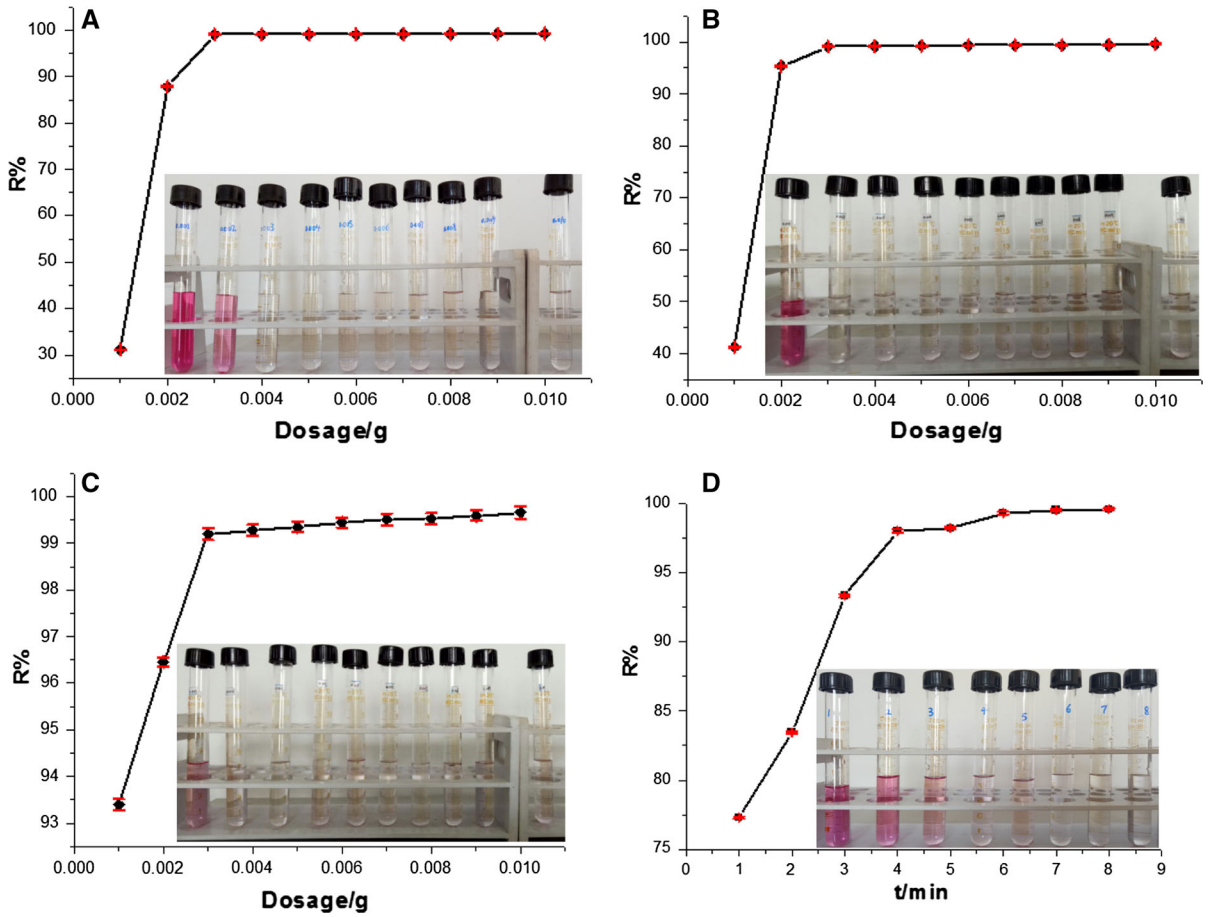

Fig. 3 Comparing the adsorption abilities of different dosages of PA-cottons at 30 °C (**a**), 40 °C (**b**) and 50 °C (**c**), and at different time (**d**). *The red marks were the error bars. The original adsorption effect at each condition could be correspondingly tracked in photos. (Color figure online)

Table 2 Comparing the adsorption capacity and rate of PA-cotton to several typical adsorbents

Adsorbent	Adsorbate	Q_{max} (mg g^{-1})	Adsorption rate (mg min^{-1} g^{-1})	References
Activated carbon	Reactive Scarlet 3BS	1.85	–	Jia et al. (2017)
Untreated cotton	Reactive Scarlet 3BS	0.20	–	Jia et al. (2017)
G-cotton	Reactive Scarlet 3BS	24.33	1.37	Jia et al. (2017)
PF-cotton	Reactive Scarlet 3BS	37.10	3.84	Jia et al. (2017)
LP-cotton	Reactive Scarlet 3BS	106.30	4.73	Song et al. (2018)
PT-cotton	Reactive Scarlet 3BS	268.82	0.72	Song et al. (2019)
PA-cotton	Reactive Scarlet 3BS	540.54	24.50	This work

Calculation methods of the adsorption rates: firstly, the mass of the adsorbed dyes could be calculated based on the adsorption results at the adsorption time when reaching the adsorption equilibrium. Subsequently, the mass of the adsorbed dyes was divided by the adsorption time and the mass of selected adsorbents to achieve the data on the adsorption rates of selected adsorbents

(natural cotton), respectively, showing an ultrahigh adsorption ability. Moreover, compared to the similar cotton-modified adsorbents developed in our previous work, i.e., G-cotton, PF-cotton, LP-cotton, and PT-cotton, the adsorption capacity of PA-cotton was improved 24.21, 14.57, 5.09, and 2.01 times. Before and after PA-cotton adsorption (Fig. 4a vs. b), there was a large colour difference (ΔE), which was measured with a Gretag Macbeth Color EYE^{R} 3100 Instrument to be 69.19, and the microscope photos of PA-cotton adsorption with a magnification of 200 × also showed that each PA-cotton fibre was fully adsorbed by the coloured dyes (Fig. 4d vs. c), directly indicating a super-high adsorption ability of PA-cotton.

Meanwhile, according to the experimental procedure in "Adsorption studies of pa-cotton samples" section, adsorption using 0.01 g PA-cottons was carried out for different lengths of time (1–8 min), and the results are shown in Fig. 3d. The results in

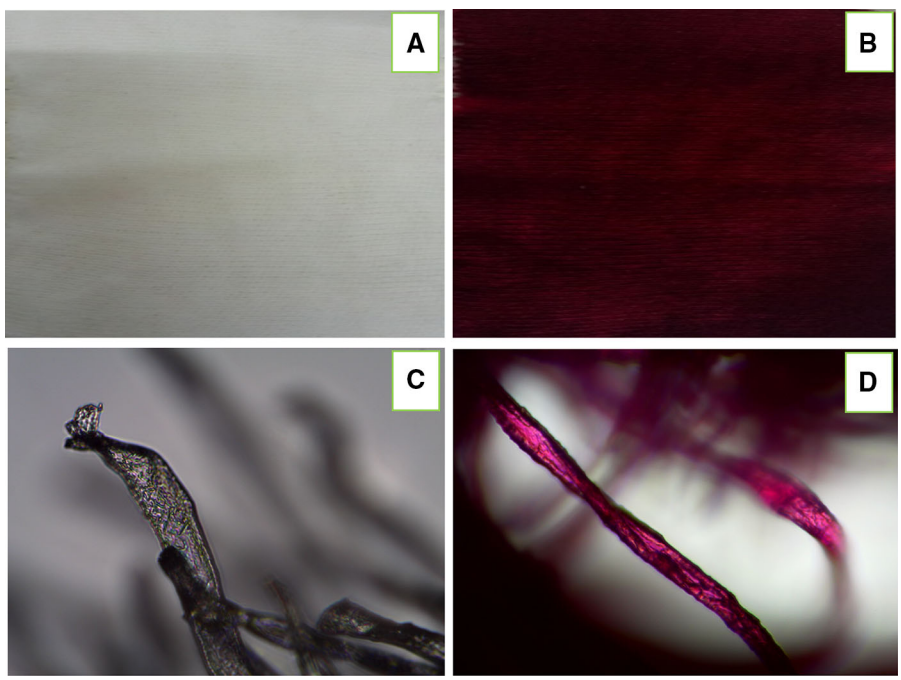

Fig. 4 The original camera photos before (**a**) and after (**b**) PA-cotton adsorption. The optical microscope photos of PA-cotton fibers before (**c**) and after (**d**) adsorbing the colored dyes (with the magnification of 200 ×)

Fig. 3d show that at a dosage of 0.01 g, it took only 4 min for the PA-cotton to adsorb 97.99% of the Reactive Scarlet 3BS dye in water, reaching adsorption equilibrium. The adsorption rate of PA-cotton was calculated as 24.50 mg min^{-1} g^{-1}, i.e., 1.00 g of PA-cottons could adsorb 24.50 mg of the anionic Reactive Scarlet 3BS dye per minute. Similar to the calculation method of PA-cotton, we further calculated the adsorption rates of the similar G-cotton, PF-cotton, LP-cotton, and PT-cotton in our previous contribution, which were 1.37 mg min^{-1} g^{-1}, 3.84 mg min^{-1} g^{-1}, 4.73 mg min^{-1} g^{-1}, and 0.72 mg min^{-1} g^{-1}, respectively (Table 2). This meant that the adsorption rate of PA-cotton was 17.88, 6.38, 5.18, and 34.03 times higher than that of the similar G-cotton, PF-cotton, LP-cotton, and PT-cotton, respectively.

Generally, through this study, both the adsorption capacity and adsorption rate of PA-cotton were respectively improved 2.01–24.21 and 5.18–34.03 times compared to those of the similar cotton-modified adsorbents in our previous work, making it possible to purify the dyeing wastewater more comprehensively than could be done before.

The recyclability of PA-cotton

According to our previous work (Jia et al. 2017), the PA-cotton adsorbed with saturated dyes could be desorbed by a 10% NaOH solution at 70 °C for 1 h (the liquor ratio, i.e., the weight ratio of NaOH solution to PA-cotton sample, was 30/1) to reform the white cotton sample similar to the primitive PA-cotton (Fig. 5a vs. a). There was a large colour difference (ΔE = 58.95) before and after PA-cotton desorption (Fig. 5a vs. b), while the colour difference between the primitive cotton and the sample after desorbing the dyes was only 10.24 (Fig. 5a vs. a), indicating that most of the adsorbed dyes had been desorbed from the PA-cotton surface.

Subsequently, the PA-cotton samples after desorbing dyes were reused to adsorb the anionic dyes in water as the process in "Structure analysis of PA-cotton" section, and the results were shown in Fig. 5b. The adsorption data of recycled PA-cotton were substituted into the Langmuir equation, and the maximal adsorption capacity (Q_{max}) of recycled PA-cotton could be calculated from the intercept of the linear plot of this equation to be 72.52 mg/g (Fig. 5c). Compared to the primitive PA-cotton, the adsorption capacity of recycled PA-cotton was clearly decreased, possibly because some of the ester linkages in the cationic AETAC units of PA-cotton were hydrolyzed during the desorption in NaOH solution, so that some of the cationic AETAC units were destroyed. However, the adsorption capacity of recycled PA-cotton was still 40.29 times higher than that of the widely-used activated carbon (1.8 mg/g) (Jia et al. 2017), showing a relatively good recyclability for purifying the dyeing wastewater.

Moreover, to the further interest, the concentrated desorption waste solution containing a lot of anionic dyes and NaOH (Fig. 5d) could be directly used to treat the heavy metal pollutants like copper (Cu^{2+}) in water, based on a self-purification process of these two wastewater sources to avoid the secondary pollution of the concentrated desorption waste-solution. In the case, when different volumes of the concentrated desorption waste solution were mixed with 50 mL 2000 mg/L $CuSO_4$ solution, it was discovered that the pollutants in these two waste solutions self-formed the insoluble flocs to be separated from water phase, so as to make water clear (Fig. 5e). As the results, on the one hand, the above 97.44% of Cu^{2+} pollutants had been removed from water phase at a large volume ratio ranges of the concentrated desorption waste solution to $CuSO_4$ solution being 1/130-1/20 (Fig. 5e). On the other hand, it was observed that the dye's absorbances (at the maximum absorbance–wavelength of the selected dye being 588 nm) when the concentrated desorption waste solutions were mixed with the $CuSO_4$ solutions according to the volume ratios being 1/130-1/40 were far lower than when the concentrated desorption waste solutions were mixed with the deionized water in the same volume ratios (Curve "b" vs. Curve "a" in Fig. 5f). According to the calculation formula in Eq. 4, the satisfactory dye removal percentages could be calculated to be 93.80–98.73% at the volume ratios being 1/130-1/40, further indicating that the desorbed anionic dyes in the concentrated desorption waste solution had been also efficiently removed from water phase. This was the first observation of self-purification of two different wastewater sources.

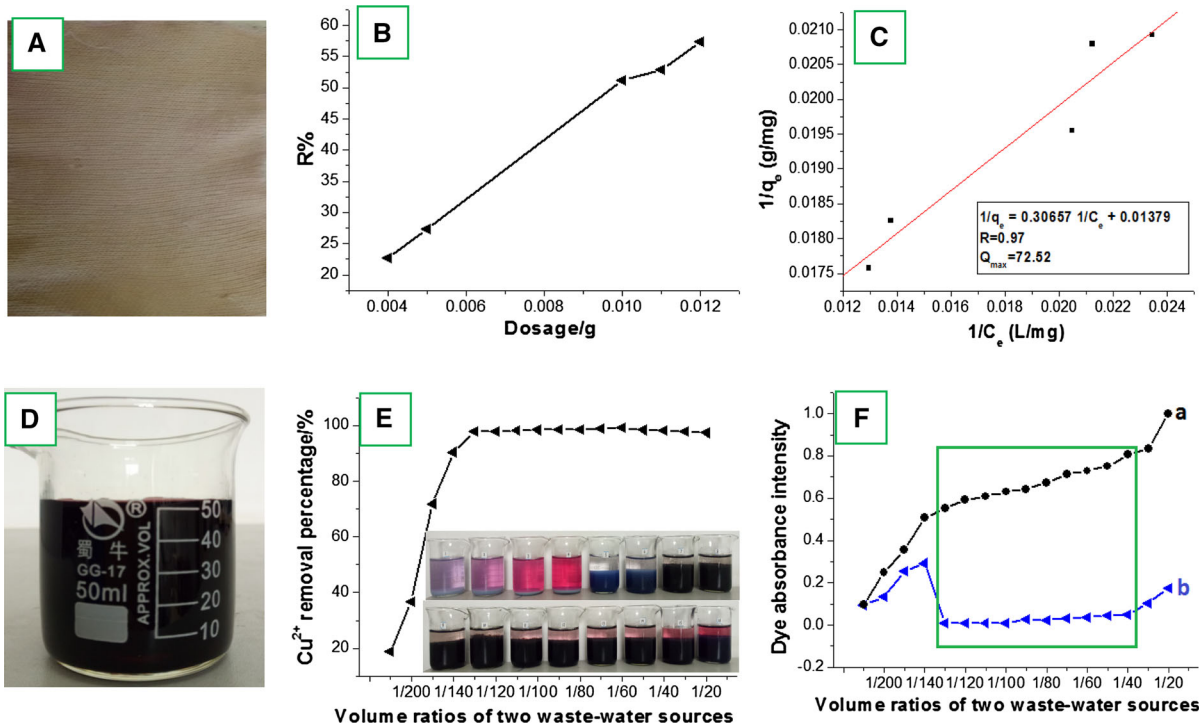

Fig. 5 Several experimental results on the recycling applications of PA-cotton. **a** The original photo of the recycled PA-cotton sample after desorbing dyes. **b** Adsorption test of recycled PA-cotton: 0.004–0.012 g of recycled PA-cottons were immersed into 10 mL of a 100 mg/L dye solution of Reactive Scarlet 3BS at 30 °C to adsorb for 100 h. **c** Fitting the Langmuir using adsorption data of recycled PA-cottons to achieve the maximal adsorption capacity (Q_{max}). **d** The original photo of the concentrated desorption waste solution derived from the PA-cotton desorption. **e** The effect of concentrated desorption waste-solution on Cu^{2+} removal in water based on the self-purification interactions of these two wastewater sources. The original interaction effect at different volume ratios of concentrated desorption waste-solution to $CuSO_4$ solution (2000 mg/L) could be correspondingly tracked in photos. **f** The effect of the self-purification interactions of two wastewater sources (concentrated desorption waste solution and $CuSO_4$ solution) on the dye removal in water

Microstructure transformations of PA-cotton adsorption for purifying dyeing wastewater

The previous FT-IR analysis after PA-cotton adsorption in Fig. 2 showed a clear information that PA-cotton could undergo a microstructure transformation after adsorbing the dyes, which had interested us to further select the XPS and XRD technologies to systemically confirm the microstructure transformations during PA-cotton adsorption in this section. The results were shown in Figs. 6 and 7, respectively.

XPS showed that compared to the analysis of PA-cotton without adsorbing the dyes (Fig. 6a–c), after adsorbing the coloured dyes of Reactive Scarlet 3BS (Fig. 6d–f), the binding energy of N 1S of PA-cotton increased from 400.16 to 402.53 eV, possibly because the *N*-containing cation of PA-cotton had formed strong binding interactions with the anionic dyes. Moreover, the binding energy of C 1S of PA-cotton was slightly shifted from 285.44 to 286.19 eV, which could possibly be derived from the induction of the C-containing flexible long-chain of PA-cotton to the adsorption of dyes in water. However, the binding energy of O 1S in the cotton skeleton of PA-cotton changed little. The above microstructure transformations further indicated that the flexible long-chain cation (i.e., AETAC unit) of PA-cotton could produce a specific inductive effect to adsorb the dyes in water.

In addition, the crystalline structures of PA-cotton when adsorbing the dyes in water were analysed by XRD (Fig. 7). The results showed that compared to the XRD spectrum of untreated cotton (Fig. 7a), there were no new crystalline peaks for PA-cotton before (Fig. 7b) and after (Fig. 7c) adsorbing the coloured dyes of Reactive Scarlet 3BS, indicating that the polycationic structures from the AETAC

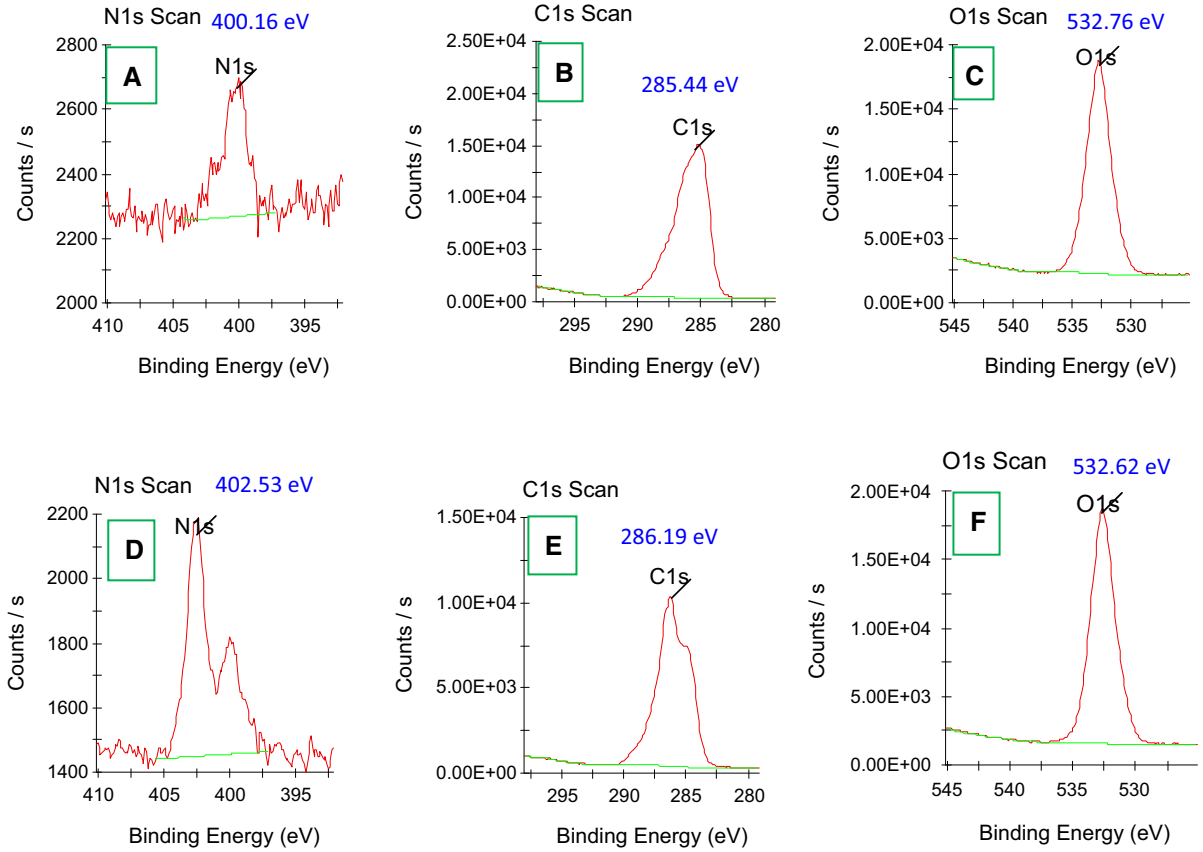

Fig. 6 Comparing XPS analysis for detecting the interaction binding energy transformations during PA-cotton adsorption. *Sample description: the PA-cotton with saturated adsorption was selected as the test sample after adsorbing the dyes, which was derived from the following adsorption conditions: 0.1 g of PA-cottons were immersed into 1.0 L of a 100 mg/L dye solution of Reactive Scarlet 3BS at 30 °C to adsorb for 100 h. **a** Scanning the binding energy of N 1s of PA-cotton before adsorbing the dyes. **b** Scanning the binding energy of C 1s of PA-cotton before adsorbing the dyes. **c** Scanning the binding energy of O 1s of PA-cotton before adsorbing the dyes. **d** Scanning the binding energy of N 1s of PA-cotton after adsorbing the dyes. **e** Scanning the binding energy of C 1s of PA-cotton after adsorbing the dyes. **f** Scanning the binding energy of O 1s of PA-cotton after adsorbing the dyes

polymerization formed on PA-cotton were amorphous, which caused the dyes to permeate inside of the PA-cotton to be adsorbed. Compared to the untreated cotton, the crystalline peaks of PA-cotton without adsorbing the dyes decreased when they were put together with those of untreated cotton (Fig. 7b vs. a), while the crystalline peaks reverted back to the original intensity, which was the same as those of the untreated cotton (Fig. 7c vs. a). This was the first discovery of the crystalline structure transformation for a cotton adsorbent to adsorb the coloured dyes in water, possibly because high density polycations formed on the surfaces of PA-cotton fibres (Scheme 3a). Therefore, each PA-cotton fiber had the same positive charges to produce the repulsive forces between each PA-cotton fibre (Scheme 3b), resulting in a decrease in the ordered alignment of each PA-cotton fibre to decrease the crystallinity of PA-cotton. After adsorbing the anionic dyes in water, the positive charges of each PA-cotton fibre were neutralized by the negative charges of the anionic dyes, resulting in a decrease in the repulsive forces between each PA-cotton fibre, increasing the ordered alignment of each PA-cotton fibre (Scheme 3c), thus re-increasing the crystallinity of PA-cotton.

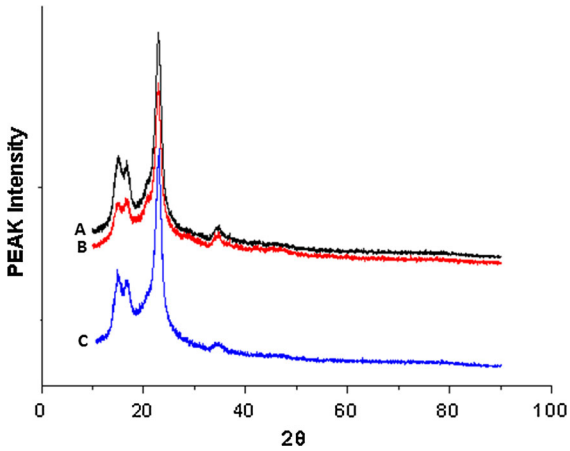

Fig. 7 Comparing XRD analysis for detecting the crystalline structure transformations during PA-cotton adsorption. **a** The XRD curve of untreated cotton, **b** the XRD curve of PA-cotton before adsorbing the dyes, **c** the XRD curve of PA-cotton after adsorbing the dyes

Adsorption models of PA-cotton based on the long-distance flexible inductive effect

In "Microstructure transformations of PA-cotton adsorption for purifying dyeing wastewater" section, there were several signs regarding the microstructure transformations of PA-cotton adsorption, indicating that the flexible long-chain cation (i.e., AETAC unit) of PA-cotton could produce a specific inductive effect to adsorb the dyes in water. To further confirm this specific inductive effect of PA-cotton, several typical adsorption isotherm models, adsorption kinetics models, and adsorption thermodynamic models were selected to further investigate the adsorption mechanisms of PA-cotton.

Adsorption isotherms of PA-cotton

Based on the experimental procedure in "Adsorption studies of PA-cotton samples" section and the data in Fig. 3a, the equilibrium adsorption (q_e) of PA-cotton and the equilibrium dye concentration in the solution (C_e) were calculated and were used to fit the typical adsorption isotherm equations (Eq. 5, Langmuir equation and Eq. 6, Freundlich equation).

$$\frac{1}{q_e} = \frac{1}{Q_{\max} K_L C_e} + \frac{1}{Q_{\max}} \tag{5}$$

$$\log q_e = \log K_f + \frac{1}{n} \log C_e \tag{6}$$

The slopes and intercepts of the liner plots of Eqs. 5 and 6 (Fig. 8) give the maximal adsorption capacity (Q_{max}), the characteristic constant of the Langmuir equation (K_L), and the characteristic constants of the Freundlich equation (K_f, n), all of which can be used to evaluate the adsorption behaviours of PA-cotton.

The results showed that the adsorption data could fit well with the Langmuir model (R = 0.90, Fig. 8a) and Freundlich model (R = 0.99, Fig. 8b), with high correlation coefficients, indicating that the adsorption

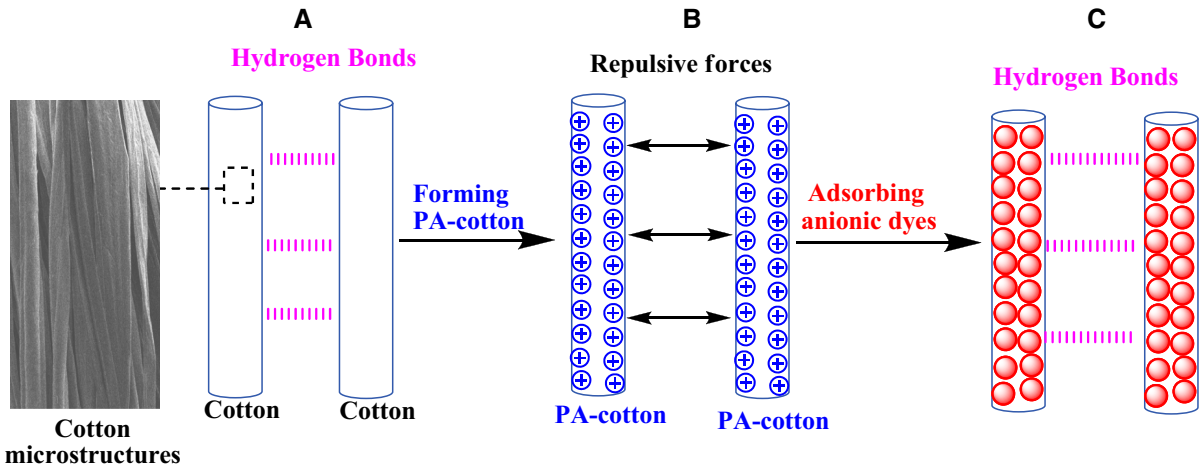

Scheme 3 The models for the crystalline structure transformations of untreated cotton (**a**), PA-cotton before (**b**), and after (**c**) adsorbing anionic dyes. Plus circle: The cationic group, red circle: The combination between the cationic group of PA-cotton and the anionic dye. (Color figure online)

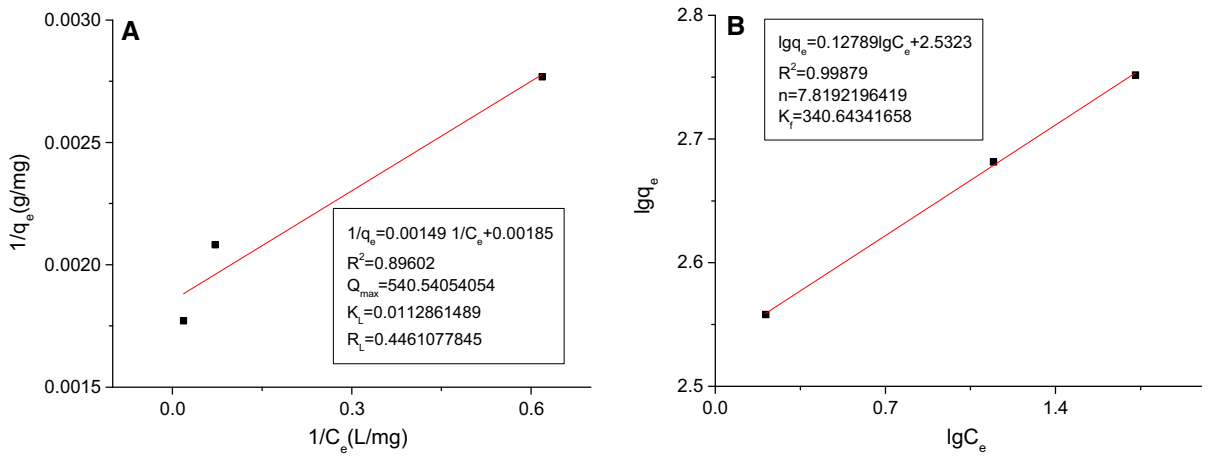

Fig. 8 Fitting the Langmuir model (**a**) and Freundlich model (**b**) using adsorption data

of PA-cotton was a typical single molecular layer adsorption process.

The dimensionless R_L constant for determining the adsorption tendency in the Langmuir model was calculated based on the characteristic constant of the Langmuir model (K_L= 0.012) using the following equation (Eq. 7):

$$R_L = \frac{1}{1 + K_L C} \tag{7}$$

The R_L value of PA-cotton adsorption was calculated as 0.45, which was a characteristic value, suggesting that PA-cotton could easily adsorb the anionic dyes in water (when $0 < R_L < 1$, adsorption can be performed easily). Moreover, the characteristic constant representing the adsorption tendency in the Freundlich equation (n = 7.82) also suggested that the adsorption of PA-cotton was very easy (when $1 < n < 10$, adsorption can be performed easily). It can be summarized from the above results that PA-cotton could easily adsorb the anionic dyes in water according to the single molecular layer adsorption process.

Adsorption kinetics of PA-cotton: the long-distance flexible inductive effect

Based on the experimental procedure in "Adsorption studies of PA-cotton samples" section and the adsorption results at different times in Fig. 3b, the dye concentration in the solution (C_t) and the amount of dye adsorption (q_t) at time t was calculated and were used to fit the typical adsorption kinetics equations (Eq. 8, pseudo-first kinetics equation; Eq. 9, pseudo-second kinetics equation; Eq. 10, intraparticle diffusion equation; and Eq. 11, particle diffusion equation).

$$\log(q_e = q_t) = \log q_e - \frac{k_1 t}{2.303} \tag{8}$$

$$\frac{t}{q_t} = \frac{1}{k_2 q_e^2} + \frac{t}{q_e} \tag{9}$$

$$q_t = k_i t^{1/2} + x_i \tag{10}$$

$$\ln\left(1 - \frac{q_t}{q_e}\right) = -k_p t \tag{11}$$

The slopes and intercepts of the liner plots of Eqs. 8–11 (Fig. 9) give the adsorption rate constants corresponding to the pseudo-first kinetics (k_1), pseudo-second kinetics (k_2), intraparticle diffusion (k_i), and particle diffusion equations (k_p), respectively, all of which can be used to evaluate the adsorption kinetic behaviours of PA-cotton.

The results showed that when the PA-cotton adsorption data fitted the pseudo-first kinetics (R = 0.94), pseudo-second kinetics (R = 0.99), and particle diffusion equations (R = 0.94), the correlation coefficients were obviously higher than when fitting the intraparticle diffusion equation (R = 0.86), indicating that the chances of adsorption on the PA-cotton surface were higher than on the inside of the PA-cotton, i.e., the long-chain cations of PA-cotton had more chances to timely catch the anionic dyes. By comparing the corresponding kinetic parameters to

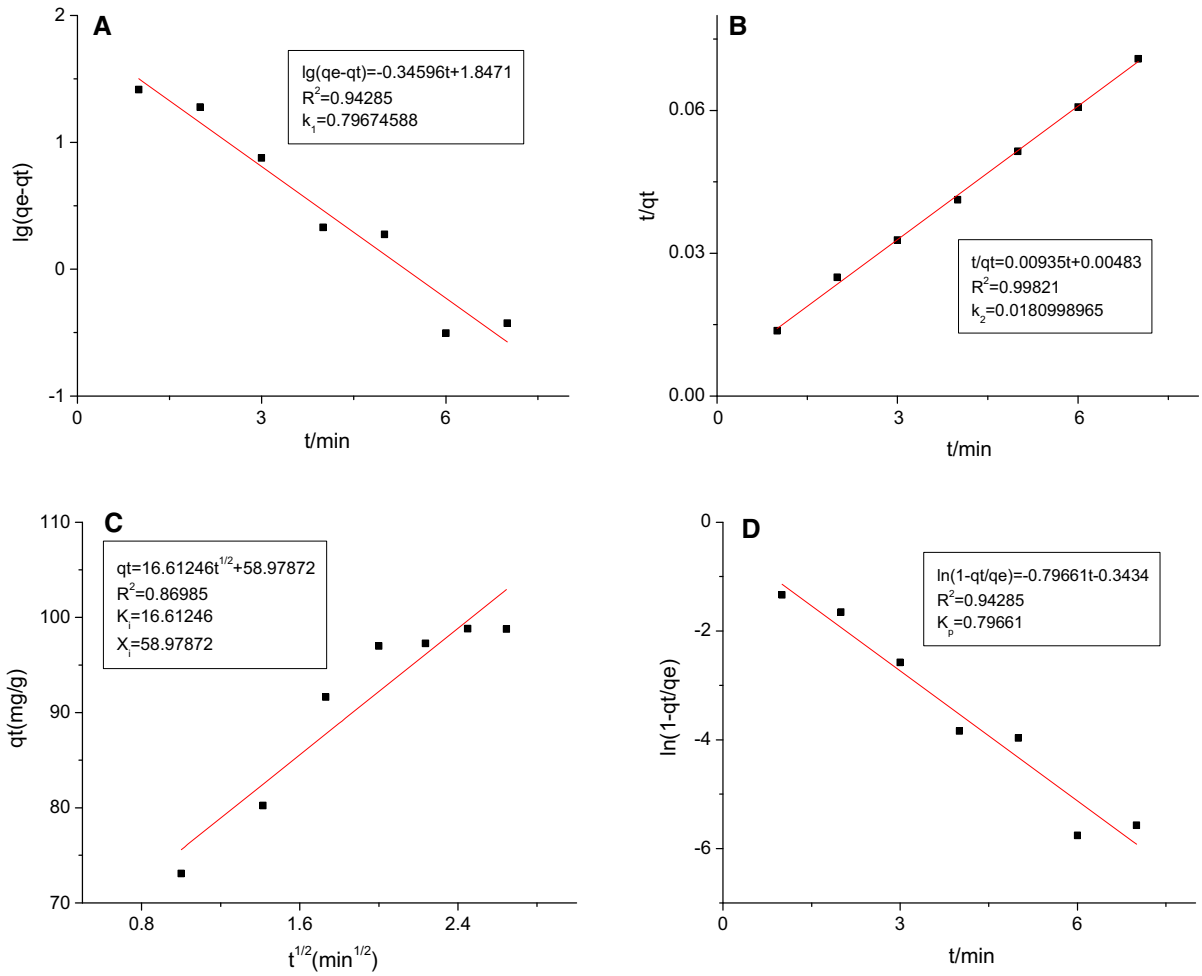

Fig. 9 Fitting the pseudo-first kinetics (**a**), pseudo-second kinetics (**b**), intraparticle diffusion (**c**), and particle diffusion equations (**d**)

those of the similar G-cotton, PF-cotton, LP-cotton, and PT-cotton in our previous work (Table 3), the interfacial thickness constant of PA-cotton (x_i= 58.98) was found to be 72.81, 14.25, 113,42, and 24.89 times higher than that of the similar G-cotton, PF-cotton, LP-cotton, and PT-cotton, respectively, indicating that the overall interfacial thickness on the PA-cotton surface is far thicker than that of the similar cotton-modified adsorbents in our previous work. This means that the long-chain linkages in the AETAC units lengthened the distance between the cations and cotton surface and the high-density polycationic coverage from the AETAC polymerization could be formed on the cotton surface, therefore, increasing the overall interfacial thickness of PA-cotton. Though the other adsorption rate constants of PA-cotton adsorption were moderate, the adsorption rate constant of PA-cotton adsorption corresponding to the intraparticle diffusion equation (k_i= 16.61 mg g^{-1} $min^{1/2}$) was 4.25, 4.93, 4.93, and 10.13 times higher that of the similar G-cotton, PF-cotton, LP-cotton, and PT-cotton, respectively, increasing the overall adsorption rate of PA-cotton because the incorporated cations of the AETAC units were flexible, having high enough mobile activities to transfer the adsorbed dyes inside the PA-cotton.

The above results confirmed that the long-chain cations could probe a far distance into the water, increasing the chances for PA-cotton to timely catch the anionic dyes without hindrance. Subsequently, the incorporated cations were flexible, having high enough mobile activities to transfer the adsorbed dyes

Table 3 Comparing the adsorption kinetics constants of PA-cotton to several similar cotton-modified adsorbents

Adsorbent	Adsorbate	K_1 (min^{-1})	K_2 (g mg^{-1} min^{-1})	K_p (min^{-1})	X_i	K_i (mg g^{-1} $min^{1/2}$)	References
G–cotton	Reactive Scarlet 3BS	0.593	0.067	0.593	0.81	3.91	Jia et al. (2017)
PF–cotton	Reactive Scarlet 3BS	1.511	0.203	1.511	4.14	3.37	Jia et al. (2017)
LP–cotton	Reactive Scarlet 3BS	0.035	0.019	0.035	0.52	3.37	Song et al. (2018)
PT–cotton	Reactive Scarlet 3BS	0.096	0.081	0.094	2.37	1.64	Additional test[a]
PA-cotton	Reactive Scarlet 3BS	0.80	0.018	0.80	58.98	16.61	This work

[a]Due to the lack of the data on the adsorption kinetics constants of PT–cotton in the previous work (Song et al. 2019), the data on the adsorption kinetics constants of PT–cotton in Table 2 were retested as follows: firstly, 0.10 g of PT–cottons were added to 10 mL of 100 mg/L dye solution of Reactive Scarlet 3BS to absorb the anionic dye in water at 30 °C for 1–10 min with the continuous stirring, respectively, and then filtered. A spectrophotometer was used to determine the dye concentration in the solution (C_t) at each time interval (t). Subsequently, the combination of the values of q_e and C_t was adopted to calculate the amount of dye adsorption (q_t) at time t. Finally, the data obtained at 1–10 min were respectively substituted into the corresponding adsorption kinetics equations to achieve the adsorption kinetics constants

into the inside of the PA-cotton, i.e., a long-distance flexible inductive effect occurred during PA-cotton adsorption, significantly raising the adsorption rate and capacity of PA-cotton, which further agreed with results from the analysis of microstructure transformations of PA-cotton adsorption in "Comparing the adsorption capacity and rate of PA-cotton" section.

Adsorption thermodynamics of PA-cotton

Based on the experimental procedure in "Adsorption studies of PA-cotton samples" section and the adsorption data at 30–50 °C in Fig. 3a–c, the dye concentration in the solution (C_e) and cotton sample (C_s, i.e., the ratio of the mass of adsorbed dyes to the solution volume) at 30–50 °C and the ratio value of C_s to C_e was calculated to obtain the equilibrium constant K_c (Eq. 12). Subsequently, the Gibbs energy ($\triangle G$) was calculated based on the numeric value of K_c (Eq. 13). Finally, the values of $\triangle H$ and $\triangle S$ were estimated from the slope and intercept of the linear plot of ln K_c versus $1/T$ (Eq. 14), and the result is shown in Fig. 10.

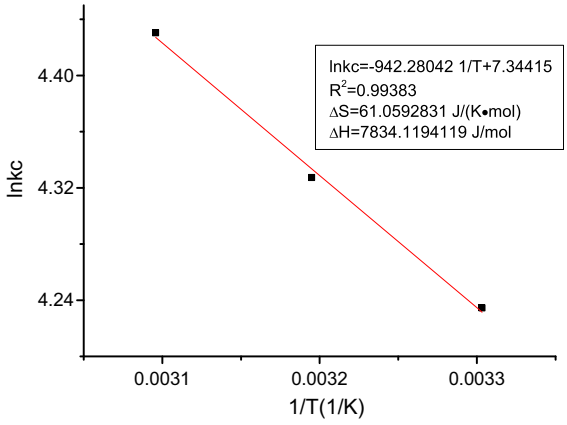

Fig. 10 Linear plot of adsorption thermodynamics of PA-cotton. *Test conditions: 0.002 g of PA-cotton samples were immersed into 10 mL of a 100 mg/L dye solution of Reactive Scarlet 3BS at 30–50°C for 100 h

$$K_c = \frac{C_s}{C_e} \tag{12}$$

$$\Delta G = -RT \ln K_c \tag{13}$$

$$\ln K_c = \frac{\Delta H}{RT} + \frac{\Delta S}{R} \tag{14}$$

K_c is the equilibrium constant of adsorption thermodynamics and ΔG, ΔH, and ΔS are the free energy, enthalpy, and entropy, respectively.

Figure 10 shows that the adsorption enthalpy (ΔH) of PA-cotton was positive (7.83 kJ/mol), indicating that the adsorption of PA-cotton was endothermic, possibly because the endothermic characteristic could improve the kinetic energy of the cations of PA-cotton. Therefore, they had enough mobile activities to increase the combination frequencies with the anionic dyes, which was in accordance with the adsorption

kinetics results of PA-cotton adsorption. According to the Gibbs free energy equation ($\Delta G = \Delta H – T\Delta S$, only when $\Delta G \leqq 0$ can adsorption could be performed spontaneously), the critical adsorption temperature of PA-cotton was calculated as − 144.57 °C, indicating that PA-cotton could effectively adsorb the anionic dyes in water at − 144.57 °C. Therefore, the adsorption of PA-cotton could occur spontaneously in the temperature environment of the earth.

Conclusion

A new PA-cotton adsorbent material was designed, which had a super-high adsorption capacity and adsorption rate for purifying dyeing wastewater. The adsorption capacity of PA-cotton was 292.18 and 2702.70 times higher than that of the widely-used activated carbon and the common natural cotton. When compared to the existing similar cotton-modified adsorbents, the adsorption capacity of PA-cotton improved 2.01–24.21 times and the adsorption rate of PA-cotton improved 5.18–34.03 times. Moreover, PA-cotton achieved a relatively good recyclability through a desorption technology, maintaining 40.29 times higher adsorption capacity than activated carbon. This was the first realization of self-purification of the desorption waste solution in this recycling application to avoid secondary pollution.

The microstructure transformations of PA-cotton adsorption were analysed by FT-IR, XPS, and XRD. The results showed that the AETAC unit of PA-cotton had a sensibility to adsorb the dyes in water. The binding energy of N 1s of PA-cotton adsorption increased from 400.16 to 402.53 eV, indicating that the N-containing cation of PA-cotton had formed strong binding interactions with the anionic dyes. Moreover, the binding energy of C 1S of PA-cotton also shifted slightly from 285.44 to 286.19 eV, which could possibly be derived from the induction of the C-containing flexible long-chain of PA-cotton to the adsorption of dyes in water, suggesting a specific inductive effect for PA-cotton adsorption. The polycationic structures from the AETAC polymerization on PA-cotton were discovered to be amorphous, which was caused the dyes to permeate inside the PA-cotton to be adsorbed. This was the first discovery of the crystalline structure transformation by XRD analysis of PA-cotton adsorption for purifying dyeing wastewater.

By studying the isotherm, kinetics, and thermodynamic models of PA-cotton adsorption, it was further confirmed that a new long-distance flexible inductive effect occurred during PA-cotton adsorption, causing it to have super-high adsorption ability. The adsorption of PA-cotton was endothermic; however, the critical adsorption temperature of PA-cotton was − 144.57 °C, i.e., PA-cotton could effectively remove the anionic dyes in water above − 144.57 °C. Therefore, the adsorption of PA-cotton could occur spontaneously in the temperature environment of the earth.

Acknowledgments This work was financially supported by the National Nature Science Foundation of China (Project No. 21866016).

References

Agbovi HK, Wilson LD, Tabil LG (2017) Biopolymer flocculants ad oat hull biomass to aid the removal of orthophosphate in wastewater treatment. Ind Eng Chem Res 56:37–46

An AK, Guo J, Jeong S, Lee EJ, Tabatabai AA, Leiknes T (2016) High flux and antifouling properties of negatively charged membrane for dyeing wastewater treatment by membrane distillation. Water Res 103:362–371

Ansari F, Ghaedi M, Taghdiri G, Asfaram A (2016) Application of ZnO nanorods looaded on activated carbon for ultrasonic assisted dyes removal: experimental design and derivative spectrophotometry method. Ultrason Sonochem 33:197–209

Aschermann G, Zietzschmann F, Jekel M (2018) Influence of dissolved organic matter and activated carbon pore characteristics on organic micropollutant desorption. Water Res 133:123–131

Chaudhary S, Kaur Y, Kumar A, Chaudhary GR (2016) Ionic liquid and surfactant functionalized ZnO nanoadsorbent for recyclable proficient adsorption of toxic dyes from waste water. J Mol Liq 224:1294–1304

Goel NK, Kumar V, Misra N, Varshney L (2015) Cellulose based cationic adsorbent fabricated via radication grafting process for treatment of dyes waste water. Carbohyd Polym 132:444–451

Gupta VK, Gupta B, Rastogi A, Agarwal S, Nayak A (2011) Pesticides removal from waste water by activated carbon prepared from waste rubber tire. Water Res 45:4047–4055

Hadi P, To MH, Hui CW, Lin CZ, Mckay G (2015) Aqueous mercury adsorption by adsorption by activated carbon. Water Res 73:37–55

Jia Q, Song C, Li H, Huang Y, Liu L, Yu Y (2017) Construction of polycationic film coated cotton and new inductive effect to remove water-soluble dyes in water. Mater Des 124:1–15

Kumar THV, Sivasankar V, Fayoud N, Oualid HA, Sundramoothy AK (2018) Synthesis and characterization of coral-like hierarchical MgO in incorporated fly ash composite for the effective adsorption of azo dye from aqueous solution. Appl Surf Sci 449:719–728

Li D, Li Q, Bai N, Dong H, Mao D (2017) One-step synthesis of cationic hydrogel for efficient dye adsorption and its second use for emulsified oil separation. ACS Sustain Chem Eng 5:5598–5607

Lompe KM, Menard D, Barbeau B (2016) Performance of biological magnetic powdered activated carbon for drinking water purification. Water Res 96:42–51

Lu S, Tang Z, Li W, Ouyang X, Cao S, Chen L, Huang L, Wu H, Ni Y (2018) Diallyl dimethyl ammonium chloride-grafted cellulose filter membrane via ATRP for selective removal of anionic dye. Cellulose 25:7261–7275

Mccleaf P, Englund S, Ostlund A, Lindegren K, Wiberg K, Ahrens L (2015) Removal efficiency of multiple poly- and perfluoroalkyl substances (PFASs) in drinking water using granular activated carbon (GAC) and anionic exchange (AE) column tests. Water Res 73:37–55

Natarajan S, Bajaj HC, Tayade RJ (2018) Recent advances based on the synergetic effect of adsorption for removal of dyes from waste water using photocatalytic process. Water Res 65:201–222

Samaneh SS, Saeed SS, Hamed JY, Mojdeh M (2017) Adsorption of anionic and cationic dyes from aqueous solution using gelatin-based magnetic nanocomposite beads comprising carboxylic acid functionalized ultrathin membranes. Chem Eng J 308:1133–1144

Shao Y, Ren B, Jiang H, Zhou B, Lv L, Ren J, Dong L, Li J, Liu Z (2017) Dual-porosity Mn_2O_3 cubes for highly efficient dye adsorption. J Hazardous Mater 333:222–231

Song C, Zhao J, Li H, Liu L, Li X, Huang X, Liu H, Yu Y (2018) One-pot synthesis and combined use of modified cotton adsorbent and flocculant for purifying dyeing wastewater. ACS Sustain Chem Eng 65:6876–6888

Song C, Yu Y, Sang X (2019) Synthesis and surface gel-adsorption effect of multidimensional cross-linking cationic cotton for enhancing purification of dyeing waste-water. J Chem Technol Biotechnol 94:120–127

Suresh P, Vijaya JJ, Kennedy LJ (2014) Photocatalytic degradation of textile-dyeing wastewater by using a microwave combustion-synthesized zirconium oxide supported activated carbon. Mater Sci Semicond Process 27:482–493

Toprak T, Anis P (2017) Textile industry environmental effects and approaching cleaner production and sustainability: an overview. J Textile Eng Fashion Technol 2:1–16

Toprak T, Anis P, Kutlu E, Kara A (2018) Effect of chemical modification with 4-vinylpyridine on dyeing of cotton fabric with reactive dyestuff. Cellulose 25:6793–6809

Wang L, Ma W, Zhang S, Teng X, Yang J (2009) Preparation of cationic cotton with two-bath pad-bake process and its application in salt-free dyeing. Carbohyd Polym 79:602–608

Wang CT, Chou WL, Chung MH, Kuo YM (2010) COD removal from real dyeing wastewater by electro-Fenton technology using an activated carbon fiber cathode. Desalination 253:129–134

Zereshki S, Daraei P, Shokri A (2018) Application of edible paraffin oil for the cationic dye removal from water using emulsion liquid membrane. J Hazard Mater 356:1–8

Zhang Y, Ma X, Xu H, Shi Z, Yin J, Jiang X (2016) Selective adsorption and separation through molecular filtration by hyperbranched poly(ether amine)/carbon nanotube ultrathin membranes. Langmuir 32:13073–13083

Zhang D, Thundat T, Narain R (2017) Flocculation and dewatering of mature fine tailing using temperature-responsive cationic polymers. Langmuir 33:5900–5909